J Appl Electrochem (2011) 41:663–668
DOI 10.1007/s10800-011-0277-0

ORIGINAL PAPER

Electrochemical fabrication of Rh–Pd particles and electrocatalytic applications

Muniyandi Rajkumar · Soundappan Thiagarajan · Shen-Ming Chen

Received: 8 December 2010 / Accepted: 27 February 2011 / Published online: 15 March 2011

Abstract Electrochemical deposition method was employed for the fabrication of rhodium–palladium (Rh–Pd) particles on the glassy carbon electrode (GCE) and indium tin oxide (ITO) electrode surface. Surface morphological analysis of Rh–Pd film has been carried out using scanning electron microscopy (SEM) and X-ray diffraction (XRD) analysis. Here, the electrodeposited Rh–Pd particles were found in the average size range of 30–200 nm. The electrochemical activities of the Rh–Pd film have been investigated using cyclic voltammetry (CV) and electrochemical impedance spectroscopic (EIS) analysis. The Rh–Pd particles-modified GCE successfully detects the hydrogen peroxide (H_2O_2) (in pH 7.0 phosphate buffer solution (PBS)) in the linear range in the lab (10–460 μM) and real samples (10–340 μM). The Rh–Pd particles-modified GCE possesses the good sensitivity and selectivity for the detection of H_2O_2 in lab and real samples.

Keywords Rh–Pd particles · Cyclic voltammetry · Amperometry · Hydrogen peroxide

1 Introduction

Bimetallic nanoparticles have made a great attention in the past decade because of their attractive physical and chemical properties and vary from their bulk metallic properties. The properties of the nanoparticles can be tuned and controlled by changing the surface morphologies or the sizes [1–7]. In recent years, bimetallic nanoparticles have an attractive area of research within nanobiotechnology and nanoelectrochemistry for their unusual optical, catalytic, and magnetic properties. Thus, bimetallic nanoparticles composed of two different metal elements are of greater interest than monometallic nanoparticles [8, 9]. Palladium (Pd) and rhodium (Rh) are the noble metals which can be crystallized with a face centered cubic (FCC) packing [10]. Recently, fabrication of noble metal nanoparticles has been found as emerging topic in nanotechnology. Different types of noble nanoparticles have been fabricated and reported. Some of the few examples based on rhodium and palladium were; reaction-driven restructuring of Rh–Pd and Pt–Pd core–shell nanoparticles [11], electrochemical preparation, and characterization of thin deposits of Pd-noble metal alloys [12] and dendrimer-Rh nanoparticle-modified glassy carbon electrode (GCE) [13].

Hydrogen peroxide (H_2O_2) has a great importance in clinical, industrial, and environmental analysis. Many methods have been used for determination of H_2O_2, such as photometry, chemiluminescence, and high performance liquid chromatography [14]. Among these methods, electrochemistry has received considerable attention due to its convenience, high sensitivity, and selectivity for the detection of H_2O_2. In general, electrodes were modified with biomolecule films [15], conducting polymers [16], redox dye [17], and nanomaterials [18]. In this nanomaterials and conducting polymers have great research interest in the fabrication of electrochemical sensor due to their versatility in the physical and chemical properties [19]. Nanomaterials have received greater attention in the field of sensors, due to their unique properties [20]. Protein- or enzyme-modified electrodes also used for amperometric

M. Rajkumar · S. Thiagarajan · S.-M. Chen (✉)
Electroanalysis and Bioelectrochemistry Lab,
Department of Chemical Engineering and Biotechnology,
National Taipei University of Technology, No.1, Section 3,
Chung-Hsiao East Road, Taipei 106, Taiwan, ROC
e-mail: smchen78@ms15.hinet.net

sensing of H_2O_2. However, the electrocatalytic activities of the enzyme- and protein-modified electrodes depend on the temperature and pH values. To overcome these obstacles, various electrode materials such as noble metal and metal oxide nanoparticles-modified electrodes were used for the direct detection of H_2O_2 [21–24]. Therefore, metal nanoparticles-modified electrodes will be promising methods for the fabrication of H_2O_2 sensors.

In this report, we have attempted to fabricate the Rh–Pd particles-modified electrodes using electrochemical deposition method for the direct detection and determination of H_2O_2. The Rh–Pd particles have been fabricated on GCE and ITO electrodes using cyclic voltammetry (CV). The surface morphologies and the electrochemical activities of Rh–Pd particles have been carried out using scanning electron microscopy (SEM), X-ray diffraction analysis (XRD), and electrochemical impedance analysis (EIS). The Rh–Pd particles successfully show the detection signals for H_2O_2 sensing in both lab and real samples. It also overcomes the interference signals and showing only H_2O_2 signals in low concentration ranges, respectively.

2 Experimental

2.1 Reagents

Potassium tetra chloropalladate (III) and Rhodium (III) chloride hydrate were purchased from Strem chemicals (USA). Hydrogen peroxide was purchased from Wako chemicals (Japan). All the other chemicals (Merck) used in this investigation were of analytical grade (99%). All the experimental solutions were prepared using double-distilled deionized water. Electrocatalytic studies were carried out in phosphate buffer solution (PBS) of pH 7.0 (prepared using Na_2HPO_4 (0.05 M) and NaH_2PO_4 (0.05 M)). Pure nitrogen gas was passed through all the experimental solutions.

2.2 Apparatus

Cyclic voltammetry (CV) was performed by a CHI 1205A electrochemical analyzer and amperometric *i–t* experiment was performed by CHI 750A analyzer. A conventional three-electrode cell were used at room temperature with glassy carbon electrode (GCE) (Surface area = 0.07 cm^2) as the working electrode, Ag/AgCl (saturated KCl) electrode as reference electrode and a platinum wire as counter electrode. The potentials mentioned in all experimental results were referred to standard Ag/AgCl (saturated KCl). Surface morphology of the film was studied by SEM (Hitachi S-3000H, Japan). Indium tin oxide (ITO) thin film coated glass electrodes have been used for SEM analysis. Electrochemical impedance studies (EIS) were performed by using ZAHNER impedance analyzer (ZAHNER Elektrik Gmbh & Co KG, Germany). The XRD experiment was done using XPERT-PRO (PANalytical B.V., The Netherlands) diffractometer using Cu K_α radiation ($k = 1.54$ Å).

2.3 Electrochemical deposition of Rh–Pd particles

The bare GCE was initially polished with 0.05 μm alumina powder on BAS polishing pad and ultrasonically cleaned in double-distilled water for a minute. Furthermore, the electrode was successfully washed with double-distilled deionized water and employed for the electrochemical deposition process. Cyclic voltammetry has been employed for the fabrication of Rh–Pd particles-modified GCE. GCE was immersed in 0.2 M H_2SO_4 solution containing $RhCl_3 \cdot xH_2O$ (10^{-3} M) and K_2PdCl_4 (10^{-3} M) and the potential scan has been applied between 1 and −0.3 V, at the scan rate of 0.1 V s^{-1} for 30 cycles. Here, the equivalent molar concentrations (10^{-3} M) of Rh and Pd precursor salts have been taken for the balanced deposition of both Rh and Pd particles. Further the Rh–Pd particles-modified GCE has been rinsed with double-distilled water and employed for the detailed electrochemical studies.

3 Results and discussion

3.1 Characterization of Rh–Pd particles

Figure 1a displays the CVs of Rh–Pd particles' electrodeposition process which begins at the positive potential of 1.0 V and ends at the −0.3 V. Here, the reduction peak of Rh–Pd particles occur at the potential of 0.23 V and the oxidation process takes place at 0.73 V. The hydrogen adsorption and desorption process takes place in the range of −0.2 to −0.13 V. For the continuous cycles, the reduction and oxidation peaks of the Rh–Pd particles were clearly increasing. This confirms that the electrodeposition of Rh–Pd particles takes place at the GCE surface. Due to the simultaneous deposition of both Rh and Pd particles in hybrid stage, we cannot distinguish the separate reduction peaks of Rh and Pd particles. Therefore, the appearance of reduction and oxidation peaks in Fig. 1a indicates the electrodeposition process of both Rh and Pd particles, respectively.

In the next step, Rh–Pd particles-modified GCE was employed for the different scan rate studies in pH 7.0 PBS. Figure 1b shows different scan rate studies of the Rh–Pd particles-modified GCE. Here, all the anodic and cathodic peak currents of Rh–Pd particles increase linearly with respect to the scan rate in the range of 0.01–1 V/s. Furthermore, the insets of Fig. 1b show the plot of cathodic

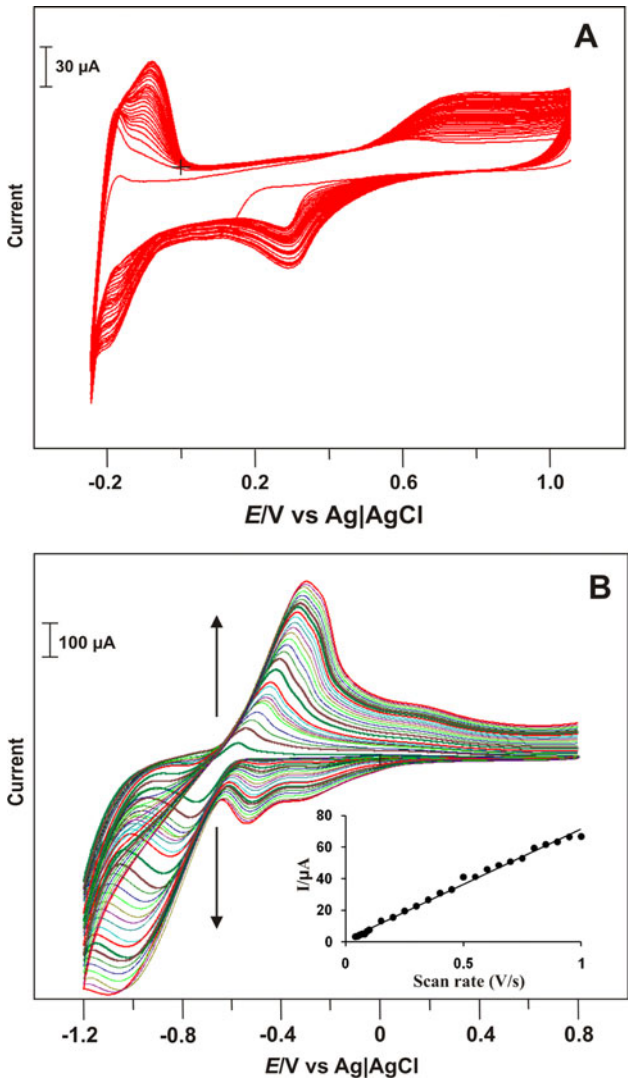

Fig. 1 **a** Consecutive cyclic voltammograms of Rh–Pd particles electrodeposited on the GCE from 0.2 M H_2SO_4 containing $RhCl_3 \cdot xH_2O$ (1×10^{-3} M) and K_2PdCl_4 (1×10^{-3} M) and potential scan between 1 to −0.3 V for 30 cycles at the scan rate of 0.1 V/s. **b** Different scan studies of the Rh–Pd particles modified GCE in pH 7 PBS at the scan rates of 0.01, 0.02, 0.03, 0.04, 0.05, 0.06, 0.07, 0.08, 0.09, 0.1, 0.15, 0.2, 0.25, 0.3, 0.35, 0.4, 0.45, 0.5, 0.55, 0.6, 0.65, 0.7, 0.75, 0.8, 0.85, 0.9, 0.95, and 1 V/s. *Inset* shows a cathodic current versus scan rate

peak current versus scan rate. The linear regression equation for the corresponding cathodic peak current was, respectively, expressed as I_{pc} (μA) = 70.185 (V/s) + 1.3749, $R^2 = 0.993$. Finally, the linear increase in the anodic and cathodic peak currents of Rh–Pd particles-modified GCE according to the scan rate illustrates that the proposed film was stable and exhibits the surface-controlled thin-layer electrochemical behavior.

Rh–Pd particles electrodeposited ITO has been examined for the SEM analysis. Figure 2a and b shows the SEM pictorial view of electrodeposited Rh–Pd particles on ITO surface. From the Fig. 2a and b, we can clearly notice the existence of Rh–Pd particles on the ITO surface. Here, the white and big size particles may resemble the nano Pd particles and remaining smaller size group of particles may resemble the Rh nanoparticles. Here, we also assume that the electrodeposited Rh–Pd particles may exist in both alloy and core–shell structure. Therefore, we partially claim that the electrodeposited particles as Rh–Pd nanoparticles. Here, the Rh–Pd particles were found in the size range of 30–200 nm. Here, the more visible bright particles fall in the higher dimensions, respectively. Finally, the above SEM result clearly illustrates the surface morphological nature of the Rh–Pd particles-modified ITO surface.

3.2 XRD and EIS analysis

XRD was utilized to study the detailed surface analysis of the Rh–Pd particles-modified ITO. Figure 3 shows the XRD spectrum obtained for the Rh–Pd particles electrodeposited on the ITO surface. In this spectrum, five

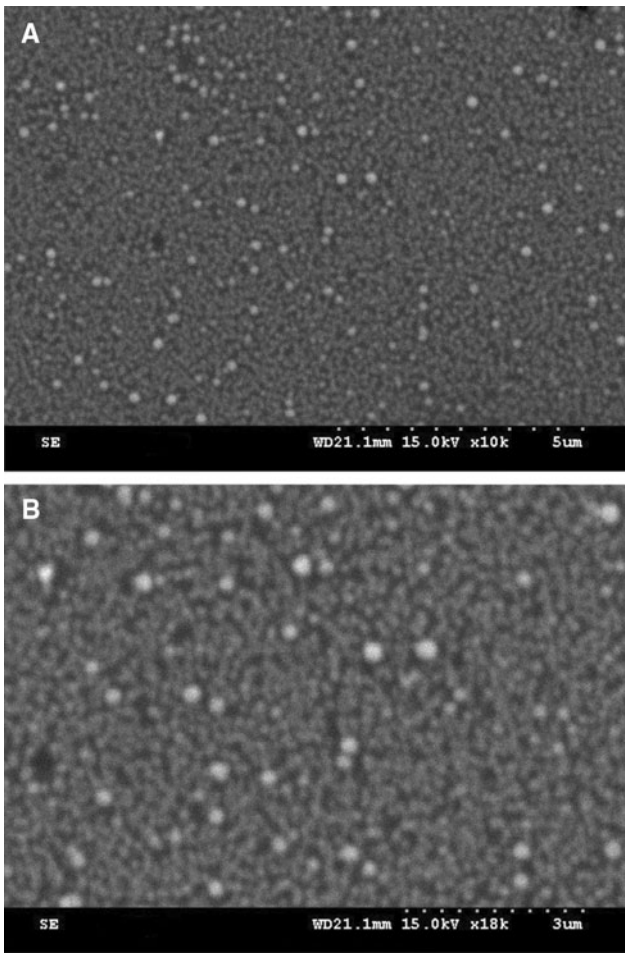

Fig. 2 SEM images of the electrodeposited Rh–Pd particles-modified ITO. Magnification **a** 5 μm, **b** 3 μm

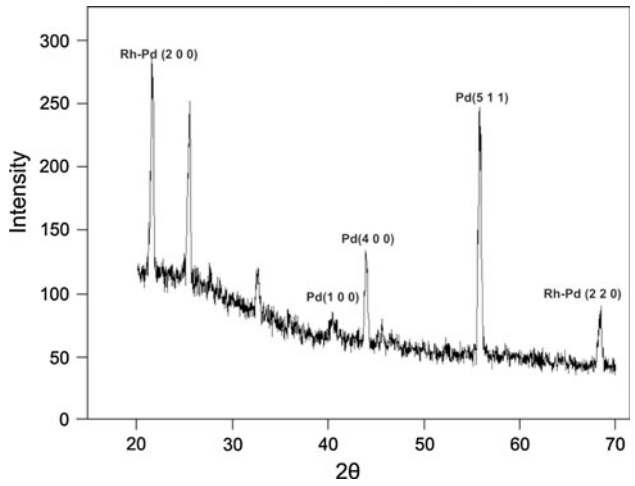

Fig. 3 XRD spectra of the Rh–Pd particles modified ITO

different characteristic peaks were obtained for the electrodeposited Rh–Pd particles. Remaining peak patterns correspond to ITO. The five characteristic peaks were Rh–Pd (200), Pd (100), Pd (400), Pd (511), and Rh–Pd (220). These five peaks clearly authenticate the presence of electrodeposited Rh–Pd particles [25, 26]. Also, here the Rh–Pd particle sizes have been calculated using the scherrer formula and this results corroborate with the SEM analysis results, respectively. Next, the electrochemical response of the Rh–Pd particles has been examined using EIS analysis. Using the EIS analysis, we can clearly analyze the electron-transfer kinetics and diffusion characteristic nature of the modified electrodes. EIS generally represents the Faradaic impedance spectra which presented as Nyquist plots (Z_{im} vs. Z_{re}) for the modified electrodes.

Here, Fig. 4 represents the Faradaic impedance spectra of bare GCE and Rh–Pd particles-modified GCE. In Fig. 4, curve a represents the response of bare GCE which displays like a very big depressed semicircle arc (R_{et} = 1900 (Z_{re}/Ω)) in pH 7 PBS containing 5 mM $[Fe(CN)_6]^{3-/4-}$. At the same time Rh–Pd particles-modified GCE exhibits like a small semicircle arc with a very low electron-transfer resistance value (R_{et} = 350 (Z_{re}/Ω)). This result shows that the Rh–Pd particles possess very good electrochemical activity comparing with the bare GCE. Therefore, this type of particles could be efficiently used for the various types of electrocatalytic reactions.

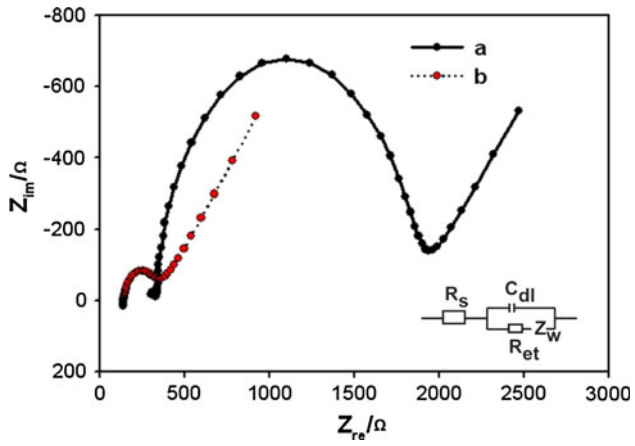

Fig. 4 EIS response of *a* bare and *b* Rh–Pd particles modified GCE in pH 7 PBS containing 5 mM $[Fe(CN)_6]^{3-/4-}$. *Inset* shows the simple Randles circuit model

3.3 Amperometric detection of H_2O_2 at Rh–Pd particles-modified GCE

Detection of H_2O_2 has been examined using CV and amperometric *i–t* techniques. At first, CV has been employed for the detection of H_2O_2. Figure 5a curve a

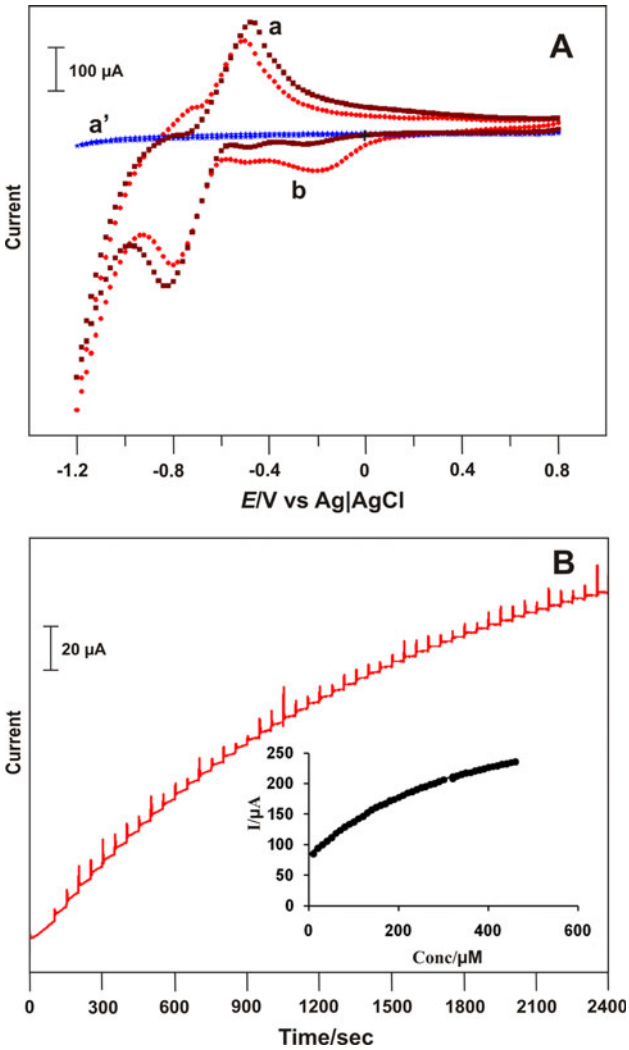

Fig. 5 **a** CV response of *a* Rh–Pd particles-modified GCE in pH 7.0 PBS, *b* in the presence of H_2O_2 (4.6×10^{-4} M, in pH 7.0 PBS) and *a′* at bare GCE, H_2O_2 (4.6×10^{-4} M, in pH 7.0 PBS). **b** Amperometric *i–t* response of Rh–Pd particles-modified GCE for the different concentrations of H_2O_2 (lab Sample) in pH 7 PBS (10–460 µM). Inset shows a current versus concentration plot of H_2O_2

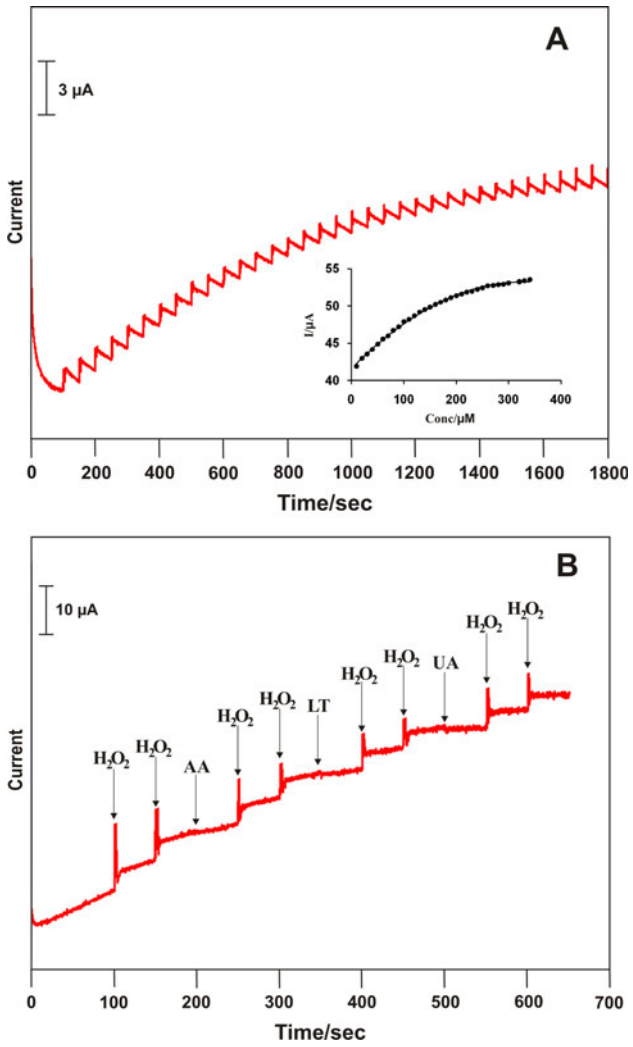

Fig. 6 **a** Amperometric *i–t* response of Rh–Pd particles modified GCE for the different concentrations of H_2O_2 (real sample) in pH 7 (10–340 μM). *Inset* shows a current versus concentration plot of H_2O_2. **b** Amperometric *i–t* response at Rh–Pd particles-modified GCE for the sequential additions of H_2O_2 (10 μM), AA, L-Tyrosine, and UA (100 μM)

shows CV response of the Rh–Pd particles-modified GCE in pH 7.0 PBS. Curve b displays the Rh–Pd particles-modified GCE response for the electrocatalytic reduction of H_2O_2 (4.6×10^{-4} M). Here, the H_2O_2 reduction signal appears at −0.17 V. At the same time, bare GCE shows diminished current response for the detection of H_2O_2 (curve a′). This shows that Rh–Pd particles-modified GCE possesses capability for detection of H_2O_2. In the next step, Rh–Pd particles-modified GCE has been employed for the amperometric detection of H_2O_2. Figure 5b shows the amperometric *i–t* response of Rh–Pd particles-modified GCE in pH 7.0 PBS for the different concentrations of H_2O_2. Rh–Pd particles-modified GCE shows the reduction current response for H_2O_2 within 5 s. Furthermore, for the increasing concentrations of H_2O_2 the electrode shows the clear response up to 460 μM. Figure 5b inset shows the current versus concentration plot of H_2O_2 detection at Rh–Pd film-modified GCE. Based on the calibration plot, the sensitivity of the proposed electrode for the H_2O_2 detection was found as 0.316 μA μM^{-1}.

In the next step, the Rh–Pd particles-modified GCE has been employed for the detection of H_2O_2 in real samples. Commercially available antiseptic solution (H_2O_2 (3%)) was used for the real sample analysis process. As expected, the Rh–Pd particles-modified GCE showed immediate electrochemical signals for the additions of the antiseptic solution within 5 s (Fig. 6a). The linear range of detection for H_2O_2 in real sample was found as 10–340 μM. Furthermore, the sensitivity of Rh–Pd particles-modified GCE for the H_2O_2 detection in real sample was found as 0.056 μA μM^{-1}. In both lab and real sample analysis, the Rh–Pd particles show excellent response for H_2O_2 detection with the good linear range and sensitivity, respectively. Therefore, this type of particles modified GCEs will be more suitable for the H_2O_2 sensors. The H_2O_2 detection at the Rh–Pd particles-modified GCE in the lab and real samples have been repeated for several times to elucidate the validity of the proposed film and the results were found satisfactory. Furthermore, Table 1 clearly shows the comparison study for the H_2O_2 detection based on the Rh and Pd particles-modified electrodes. From this Table 1, we can see that the proposed particles modified GCE possess the sufficient capability for the detection of H_2O_2.

3.4 Interference and stability studies

Interference studies for the detection of H_2O_2 at Rh–Pd particles-modified GCE have been carried out with three

Table 1 Comparison table for H_2O_2 detection using various methods and in various samples

Type of film	Linear range	Sensitivity	References
Dendrimer-Rh nanoparticle/GCE	8–30 μM	0.03103 μA μM^{-1}	[13]
Pd nanocomposite/GCE	–	656.06 mA M^{-1} cm^{-2}	[27]
Au/poly acrylic acid-Pd^0 electrode	10 μM–25 mM	232 μA mM^{-1} cm^{-2}	[28]
Nafion-MWCNTs-Pd/GCE	1.0 μM–10 mM	23 μA μM^{-1}	[29]
Rh–Pd particles/GCE	10–460 μM (lab sample)	0.3160 μA μM^{-1}	This work
	10–340 μM (real sample)	0.0560 μA μM^{-1}	

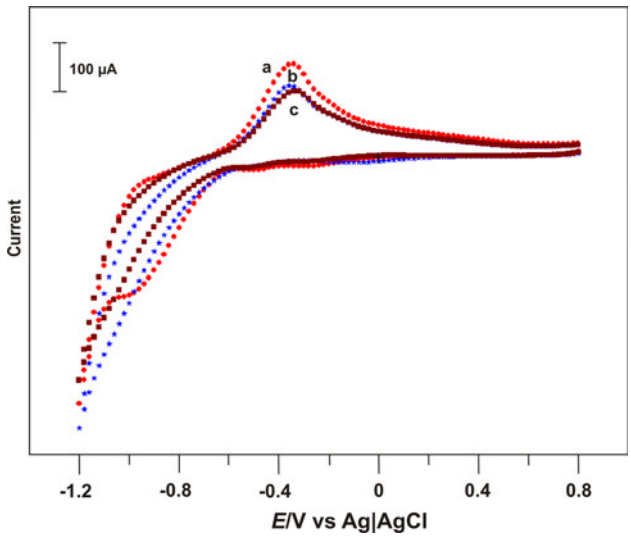

Fig. 7 CV response of Rh–Pd particles-modified GCE in the pH 7.0 PBS: *a* first day, *b* after 3 h, and *c* second day

different compounds (Fig. 6b). Ascorbic acid (AA), uric acid (UA), and L-tyrosine (LT) were used to examine the selectivity of the Rh–Pd particles-modified GCE for the detection of H_2O_2. Here, the target analyte and interfering compounds' concentration ratio were fixed as 1:10 ratio (H_2O_2 (10 μM) and AA, UA, and LT (100 μM)). No current response was observed for the injection of these compounds (AA, UA, and LT). Even in this concentration range, the Rh–Pd particles-modified GCE overcomes the interference signals and clearly shows the H_2O_2 detection signal at the various intervals, respectively.

This shows that the Rh–Pd film specifically holds the capacity to detect H_2O_2 in low concentration ranges in the presence of interfering compounds. The interference result clearly explicates that the Rh–Pd particles are appropriate and well suit for the fabrication of H_2O_2 sensors. Stability of the Rh–Pd particles-modified GCE was investigated by storing it in air at 4 °C and further checking the background current response in pH 7.0 PBS. It was stable for 2 days and few gradual decreases occurred in the reduction and oxidation peak potentials (Fig. 7). Further by increasing the number of cycles and other factors, we can improve the stability of this type of particles modified electrodes.

4 Conclusion

In conclusion, Rh–Pd particles have been successfully fabricated using the cyclic voltammetry. Fabricated particles have been examined using SEM. Electrochemical activities of the Rh–Pd particles-modified GCE have been examined using CV and EIS analysis. Rh–Pd particles-modified GCE successfully employed for the detection of the H_2O_2 in pH 7.0 PBS. It also overcomes the interference substances' signals and shows only the H_2O_2 reduction current response. Not only limited to lab sample, the proposed particles' modified GCE also employed for the detection of H_2O_2 in real samples. Based on these results, we conclude that the Rh–Pd particles could be employed as the electrochemical sensor for the detection and determination of H_2O_2.

Acknowledgment This work was supported by National Science Council (NSC) of Taiwan (ROC).

References

1. Xu CX, Wang LQ, Wang RY et al (2009) Adv Mater 21:2165
2. Chiang WH, Sankaran RM (2008) Adv Mater 20:4857
3. Luo J, Wang L, Mott D et al (2008) Adv Mater 20:4342
4. Schrinner M, Proch S, Mei Y et al (2008) Adv Mater 20:1928
5. Gunawidjaja R, Peleshanko S, Ko H et al (2008) Adv Mater 20:1544
6. Zhang QB, Xie JP, Liang J et al (2009) Adv Funct Mater 19:1387
7. Obradovic MD, Tripkovic AV, Gojkovic SL (2009) Electrochim Acta 55:204
8. Pande S, Ghosh SK, Praharaj S et al (2007) J Phys Chem C 111:10806
9. Pande S, Jana S, Sinha AK et al (2009) J Phys Chem C 113:6989
10. Lim B, Xiong Y, Xia Y (2007) Angew Chem Int Edit 46:9279
11. Tao F, Grass ME, Zhang Y et al (2008) Science 322:932
12. Łukaszewski M, Czerwiński A (2010) Thin Solid Films 518:3680
13. Chandra S, Lokesh KS, Nicolai A et al (2009) Anal Chim Acta 632:63
14. Yi X, Huang XJ, Hong YC (1999) Anal Chim Acta 391:73
15. Tang JL, Wang BQ, Wu ZY et al (2003) Biosens Bioelectron 18:867
16. Xu Q, Zhu JJ, Hu XY (2007) Anal Chim Acta 597:151
17. Salomi BSB, Mitra CK (2007) Biosens Bioelectron 22:1825
18. Liu Y, Lei JP, Ju HX (2008) Talanta 74:965
19. Sharma AK, Vatsyayan P, Goswami P et al (2009) Biosens Bioelectron 24:2313
20. Katz E, Willner I, Wang J (2004) Electroanalysis 16:19
21. Zhao B, Liu Z, Liu G et al (2009) Electrochem Commun 11:1707
22. Liu A, Dong W, Liu E et al (2010) Electrochim Acta 55:1971
23. Song MJ, Hwang SW, Whang D (2010) Talanta 80:1648
24. Zhang L, Zhai Y, Gao N et al (2008) Electrochem Commun 10:1524
25. Jeon YT, Lee GH (2008) J Appl Phys 103:094313
26. Bai Z, Yang L, Zhang J et al (2010) Catal Commun 11:919
27. Kong L, Lu X, Bian X et al (2010) Langmuir 26:5985
28. Tang Y, Cao Y, Wang S et al (2009) Sens Actuator B Chem 137:736
29. You JM, Jeong YN, Ahmed MS et al (2011) Biosens Bioelectron 26:2287